Rev Anal Chem 31 (2012): 15–28 © 2012 by Walter de Gruyter • Berlin • Boston. DOI 10.1515/REVAC.2011.120

Dielectric coated plasmonic interfaces: their interest for sensitive sensing of analyte-ligand interactions

Sabine Szunerits[1,*], Atef Shalabney[2], Rabah Boukherroub[1] and Ibrahim Abdulhalim[2,3,*]

[1] Institut de Recherche Interdisciplinaire (IRI, USR 3078), Université Lille 1, Parc de la Haute Borne, 50 Avenue de Halley, BP 70478, 59658 Villeneuve d'Ascq, France, e-mail: sabine.szunerits@iri.univ-lille1.fr
[2] Department of Electro Optic Engineering and The Ilse Katz Institute for Nanoscale Science and Technology, Ben Gurion University of the Negev, Beer Sheva 84105, Israel
[3] School of Materials Science and Engineering, Nanyang Technological University, 637722, Singapore

*Corresponding author

Abstract

Surface plasmon resonance (SPR) sensors have matured over the last 2 decades into very powerful tools for the study of biomolecular interactions, chemical detection and immunoassays. The performance of the sensor depends on several parameters, such as the choice of the metal thin film where the plasmonic wave propagates, the excitation wavelength and the refractive index (RI) of the glass prism. Next to these physical parameters, the strategy selected to bind the desired receptors to the SPR chip, has a strong influence on the overall sensitivity and selectivity of the device. This review focuses on the advancement made using lamellar SPR structures, where a thin dielectric layer is deposited onto the surface plasmon active metal thin film. Silver-based SPR interfaces can be developed using this approach, as these overlayers allow an efficient protection of the underlying silver film. At the same time, these interfaces open the scope for new surface functionalization schemes, which can be employed for anchoring ligands to the SPR sensor chip. While self-assembled monolayers (SAMs) are widely used, due to the possibility of easily incorporating carboxylate, amine or hydroxyl groups, the drawbacks of such films include limited chemical and electrochemical stability. Moreover, a poor orientation and potential problems of protein adsorption and fouling, is often encountered if no synthetic effort in the synthesis of more sophisticated thiols is made. In addition, while the surface chemistry developed on gold has been of great value, the limitations of working on gold are becoming more noticeable, with increasingly complex fabrication requirements for biometric systems and arrays. Lamellar SPR interfaces represent an alternative route. Finally, the contribution of the thin dielectric top layer to the sensitivity of SPR sensors will be discussed.

Keywords: dielectric overlayer; plasmonic; sensitivity.

Introduction

Biosensors based on the detection principle of surface plasmon resonance (SPR), are nowadays routine analytical tools for investigating ligand-analyte interactions. They are employed in areas ranging from medical diagnostics, to sensing of living cells (Chabot et al. 2009) and the detection of low levels of *Escherichia coli* (Linman et al. 2010) and serotyping of *Salmonella* (Mazumdara et al. 2010). In a SPR device, surface plasmons are used to probe the binding of target molecules, the analytes, contained in a liquid phase, to their affinity partners, the ligands, immobilized on the SPR chip. The capture of the analyte leads to a local increase in the refractive index (RI), or a change in the optical density, which induces specific alternations in the surface plasmon resonance characteristics. In fact, near the surface plasmon resonance angle, an extremely strong evanescent field is generated at the metal/dielectric interface by the surface plasmon wave. The unique characteristic of the generated evanescent field, where the field amplitude is greatest at the interface and exponentially decays as a function of distance from the metal/dielectric interface, makes the SPR signal very sensitive to RI changes in the vicinity of the metal surface. These changes are recorded commonly, using one of the three operation modes: (a) angle resolved, (b) wavelength resolved, and (c) imaging. In the first two modes, one measures the reflectivity of light from the metal surface as a function of either wavelength (at constant incidence angle) or as a function of incidence angle (at constant wavelength). The third mode uses light of constant wavelength and wide incidence angles range to interrogate a two-dimensional region of the sample, mapping the reflectivity of the sample as a function of position (Karabchevsky et al. 2011a,b).

The qualities of a SPR sensor, such as sensitivity and selectivity, are defined by the chemical and optical stability of the metal and sensing layer, as well as by the dip depth and width of the sensor signal. The sensor's sensitivity is commonly defined as the ratio between the resonance angle or wavelength shift per analyte RI. Gent et al. (1990) defined the sensitivity as the ratio between the shift and width of the SPR dip. Occasionally, the expression "sensitivity", is

misleadingly used in place of the limit of detection (LOD) of the sensor. While the sensitivity of the sensor is solely determined by the physical characteristics of the device, the LOD is defined both by the sensitivity and the noise level of the sensor as a system. The different definitions of SPR sensitivity are formally detailed and mathematically described in the second section.

Many methods were proposed to enhance the physical sensitivity of the SPR sensor, namely, enhancing the response of the sensor to variations in the analyte region (Shalabney and Abdulhalim 2011). Some of the prominent approaches of sensitivity enhancement are: decreasing the prism RI in the Kretschmann configuration in both spectral (Yuk et al. 2006) and angular interrogation (Gupta and Kondoh 2007), modifications of the metal layer by using different alloys or bimetallic structures (Yuan et al. 2006), addition of gratings on top of the dielectric layer (Jory et al. 1994, Schroter and Heitmann 1999, Zhaoming 2000, Masale 2003, Alleyne et al. 2007), using columnar thin films as the metal transducer layer (Kabashin 2009, Shalabney 2009, Shalabney 2011), using phase sensitive SPR (Kabashin and Nikitin 1998, Lee et al. 2007, Meunier et al. 2010) and many others. Since the SPR is accompanied by an enhanced evanescent field in the metal-analyte interface region, the sensor sensitivity for a perturbation in the analyte is determined by the field distribution in this region (Abdulhalim 2007). This fact was recently examined and verified by Shalabney and Abdulhalim (2010) for many of the aforementioned sensitivity enhancement methods.

The detection of small molecules and the analysis of samples with very low concentrations of analyte, remain a challenge for SPR biosensors. The smallest detectable (LOD) biomolecular weight commonly reached using SPR sensors is ≈180 g/mol (Chabot et al. 2009). In terms of mass loading, this sensitivity corresponds to a detection limit of 10 pg/mm (Linman et al. 2010). This level of LOD for a real-time, label-free optical biosensor system is still unmatched. However, in the last 2 decades, several approaches were proposed to improve the SPR sensor sensitivity by improving the resolution of SPR-based measurements of RI changes, as well as towards amplification of the sensor response. Amplification approaches exploiting labeling with gold nanoparticles, chromophores and enzymatic reactions, allowed pushing the detection limit by several orders of magnitude (Karlsson and Stahlberg 1995, He et al. 2000). The use of gold nanoparticles as labels, allowed for the detection of DNA hybridization at concentrations as low as 10 pM (Phillips and Cheng 2007). The detection of DNA at a level of 100 fM was achieved through chromophore-labeling and surface plasmon-enhanced fluorescence spectroscopy (SPFS) (Yao et al. 2004, Dostalek and Knoll 2008). However, while low detection limits can be reached with these combined approaches, the label-free character of the SPR method is lost.

One of the most promising novel structures in SPR sensors is an optical multilayer structure supporting long range surface plasmons (LRSPs). LRSPs represent a special surface plasmon mode, which can be generated when a thin metal film is sandwiched between two dielectric media of similar refractive indices. This special mode can be optically excited in a modified Kretschmann geometry, where a dielectric film whose RI is similar to that of the sensed medium is stacked between the high RI prism and the metal layer. Optical field enhancement due to LRSPs has been shown to be an order of magnitude larger than conventional surface plasmons (Sarid et al. 1982). Compared to conventional surface plasmons, LRSPs also have lower propagation loss and longer field penetration. The lower propagation loss of LRSPs leads to a narrower resonance, and the longer field penetration of LRSPs is particularly favorable for the detection of large-size analytes such as bacteria, viruses, and spores. Therefore, SPR sensors employing LRSPs are expected to offer better performance compared to sensors with conventional surface plasmons. The exploitation of long range surface plasmons for high resolution SPR sensor was first reported in 1990 (Matsubara et al. 1990). Further improvement of LRSP-based SPR sensors resulted in a RI resolution as small as 5×10^{-8} refractive index unit (RIU) and sensitivity as high as 59,000 nm/RIU (Slavik and Homola 2007, Vala et al. 2009). Lately, the combination of the conventional Kretschmann geometry with metamaterials has been shown to significantly improve the performance of SPR sensors. The use of an array of gold nanorods instead of a continuous gold film in the Kretschmann geometry resulted in enhanced SPR performance. A RI sensitivity as high as 32,000 nm/RIU has been experimentally demonstrated (Kabashin et al. 2009).

A different approach is based on the formation of lamellar SPR sensor chips as shown in Figure 1. The sensor chip configuration is similar to the conventional Kretschmann configuration, with an additional dielectric layer present on top of the metallic thin film where the surface plasmon wave is generated. The RI of the overlayer varied between n=1.48 and 2.6 and the thickness of the films between 5 and 40 nm depending, on the overlayer. Such a configuration has several advantages: firstly, the stability of the metal layers could be improved as the overlayer serves as a protection layer.

Gold is the substrate of choice for SPR measurements, as it is relatively stable in aqueous environments required for monitoring biomolecular interactions and can be easily functionalized through the formation of alkanethiols self-assembled monolayers (SAMs). However, while gold gives rise to large angular sensitivity, it is not the best candidate for achieving highly sensitive spectral sensing. Theoretical modeling of SPR in conducting metal oxide thin films has been performed by Franzen (2008) who suggested that

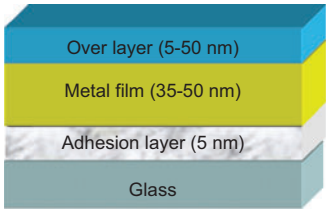

Figure 1 Schematic illustration of SPR lamellar structure of dielectric-on-gold substrate.

indium tin oxide (ITO) could be a better suited substrate (Franzen 2008). However, this would require excitation and detection in the infrared range. In the conventional visible range, silver substrates appear to be the best candidate, because plasmon coupling exhibits a sharper angular resonance as compared to that on gold, yielding an increased specular sensitivity (Liu et al. 2010). However, silver suffers from a poor chemical stability, which hampers its wide use for SPR sensing. One strategy to circumvent this limitation is to use bimetallic silver/gold layers (Zynio et al. 2002, Wang et al. 2009). Alternatively, lamellar structures were developed (Szunerits and Boukherroub 2006b, Szunerits et al. 2006, 2008c, Manesse et al. 2008a,b, 2009, Touahir et al. 2010, Maalouli et al. 2011). These overlayers allow an efficient protection of the underlying silver film. At the same time the scope for new surface functionalization schemes, which can be employed for anchoring ligands to the SPR sensor chip, is widened.

In this review, we summarize the current state of the art in the development and use of lamellar based SPR biochips. The effects of adding nano-top dielectric film coatings onto the metal films where the plasmon is generated on sensitivity and the overall performance of the plasmonic sensor will be discussed theoretically following recently published approaches used by some of us (Lahav et al. 2008, 2009). Since SPR is accompanied by an enhanced evanescent field in the metal/dielectric/analyte interface region, the sensor sensitivity for a perturbation in the analyte is determined by the field distribution in this region. This will be additionally considered. The technique of SPR becomes interesting when the metallic film, supporting the propagation of charge density waves (the plasmons), is chemically modified. We will describe the differently developed surface functionalization schemes together with some appropriate analytical examples.

Addition of nano-top dielectric film above metal: theoretical aspects

Propagating SPR at the metal/analyte and metal/dielectric/analyte interface

A short description of the SPR phenomenon and in particular, the different definitions of the sensor sensitivity, is presented. While these considerations are widely covered in many books (Schasfoort and Tudos 2008), certain points need to be well addressed in the context of sensitivities, definitions and their appropriate mathematical expressions. Surface plasmon waves (SPWs) are longitudinal charge density distributions generated on the interface between a metal and a dielectric when light propagates through the metal. The metal RI is defined as $n_m=\sqrt{\varepsilon_m}$ and the analyte/sensing medium RI is $n_a=\sqrt{\varepsilon_a}$ with ε_m and ε_a being the permittivity of the metal and the analyte, respectively. In order to generate a charge density at the interface, the incident wave should be transverse magnetic (TM) polarized, namely the magnetic field should lay in the y direction (Figure 2A). The last requirement constitutes the first condition of exciting SPW, and the fields in both the metal and the sample region can be expressed as follows:

$$E_i(r,t)=(E_{ix},0,E_{iz})e^{-k_{zi}|z|}e^{i(k_{xi}x-\omega t)}$$
$$H_i(r,t)=(0,H_{iy},0)e^{-k_{zi}|z|}e^{i(k_{xi}x-\omega t)} \quad (1)$$

where k_{zi} is the Z component of the wave vector in the layer i, and k_{xi} is the X component of the wave vector. Substituting the fields from Eq. (1) into Maxwell's equations and applying the continuity conditions and the relationship between k_{xi} and k_{zi}, results in the surface plasmon K-vector (Eq. 2), where ω is the plasma frequency and c the speed of light:

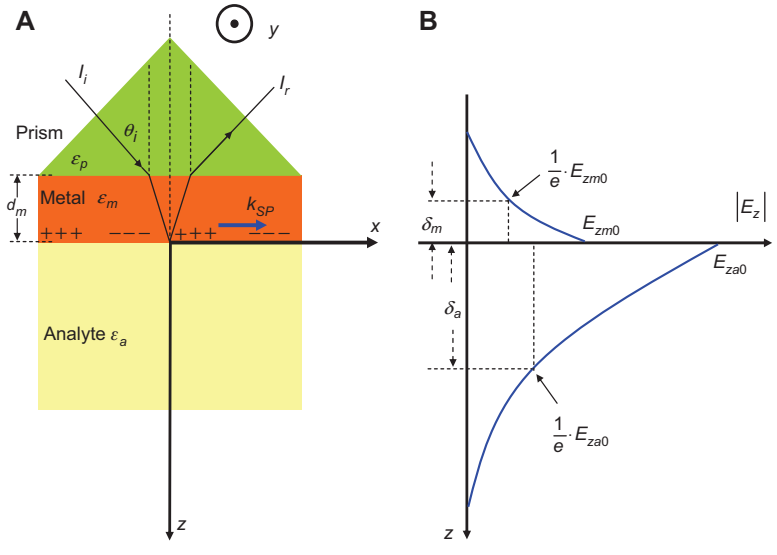

Figure 2 (A) Schematic illustrations to the longitudinal charge density generated at the metal\dielectric interface in the Kretschmann configuration. (B) Enhancing the field component perpendicular to the interface due to the surface charge. δ_m, δ_d, are the decay lengths of the field perpendicular to the surface in the metal and the dielectric regions respectively. ε_p Prism permittivity, θ_i incidence angle inside the prism, and d_m is the metal layer thickness.

$$k_{SP}=\frac{\omega}{c}\sqrt{\frac{\varepsilon_m\varepsilon_a}{\varepsilon_m+\varepsilon_a}} \tag{2}$$

Eq. (2) represents the dispersion relation of the SP, which leads to the second condition of the SP excitation (Raether 1988). Since the X-component of the incident k-vector (k_x) should coincide with k_{SP}, the condition described in Eq. 2 cannot be satisfied if the incident light (Ii) emerges from air. Therefore, the incident k-vector is enhanced by the high RI of the prism in order to fit the SP k-vector generated at the metal/dielectric interface (Figure 2A). As the permittivity of the metal and the analyte are complex ($\varepsilon_m=\varepsilon_{mr}+i\varepsilon_{mi}$ and $\varepsilon_a=\varepsilon_{ar}+i\varepsilon_{ai}$), k_{SP} is also complex and k_{zi} is pure imaginary, which means that the waves decay exponentially when both propagate inside the analyte and along the interface. Figure 2B describes the behavior of the Z component of the fields inside the metal and inside the analyte. When the conditions for SP excitement are fulfilled, a dip is obtained in the reflectivity $R=I_r/I_i$ (I_i – the incidence intensity, I_r – the reflected intensity). Eq. (2) with $k_x=k_0 n_p \sin\theta_i=k_{SP}$ yields the resonance angle when the wavelength is fixed and the resonance wavelength when the angle is fixed.

Angular sensitivity

Different definitions of the sensitivity were considered in the literature. As all our experiments were performed using a fixed wavelength, only the angular sensitivity will be considered. This is defined as the ratio between the resonance angle shift and the analyte RI change, as seen in Figure 3. Eq. 3 gives the analytical expression for the angular sensitivity for the Kretschmann configuration:

$$S_\theta\equiv\frac{d\theta}{dn_a}=\frac{\varepsilon_{mr}\cdot\sqrt{-\varepsilon_{mr}}}{(\varepsilon_{mr}+n_a^2)\cdot\sqrt{\varepsilon_{mr}(n_a^2-n_p^2)-n_a^2\cdot n_p^2}} \tag{3}$$

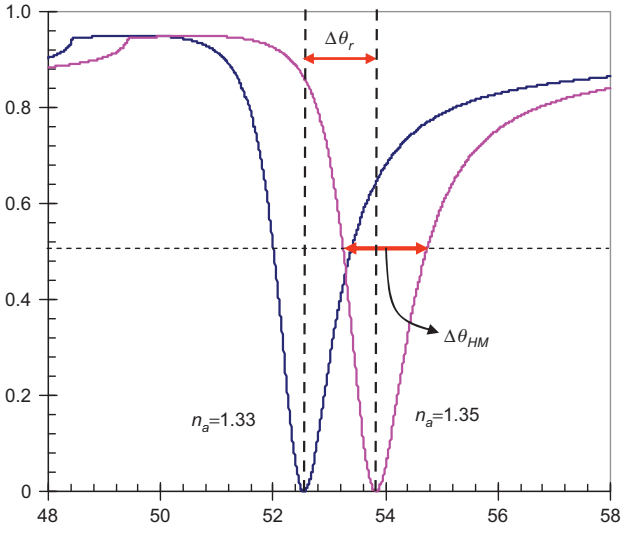

Figure 3 Change in surface plasmon resonance signal due to a change in the analyte refractive index: n_a=1.33 (blue), n_a=1.35 (pink).

where n_p, n_a are the prism and analyte refractive indices, respectively, and ε_{mr} is the real part of the dielectric constant of the metal.

The angular sensitivity, as defined above, should be distinguished from the LOD. The LOD is the smallest quantity of change in the analyte RI (or translated into concentration) that can be detected by the plasmonic system. While the sensitivity is determined solely by the transduction mechanism, the LOD is determined both by the sensitivity and the noise level of the SPR sensor, which can be highly dependent on the surface chemistry used to link the ligand. With ΔX being the change in the SPR angle and S_x the sensitivity corresponding to the parameter X, the LOD is correlated to the sensitivity of the SPR sensor by:

$$\mathrm{LOD}=\Delta X_{\min}/S_x \tag{4}$$

The parameter $\Delta X_{\min}$ is the minimum detectable angular change which is usually taken as the value of the noise level (signal-to-noise ratio SNR=1). By improving the system precision, the LOD can hence be improved. This, of course, can be achieved by several means such as using less noisy detectors and sources or by employing signal processing techniques. Lahav et al. (2008) used a parabolic fit of the neighborhood of the SPR minimum to achieve sub-pixelling and improve the LOD.

Figure of merit (FOM)

The overall performance of any SPR sensor is determined by a combination of two SPR characteristics: (i) the shift in resonance angle ($\Delta\Theta_r$) for a given change (Δn_a) in the analyte layer RI, which should be as large as possible; (ii) the full width half maximum (FWHM) corresponding to the SPR curves ($\Delta\theta_{HM}$) which should be as small as possible, so that the error in determining the resonance angle is minimal. Since a trade off usually occurs between the dip shift and width, the two parameters are taken into account by means of defining a figure of merit (FOM), defined as the ratio between the shift in the resonance angle and the FWHM of the dip (Eq. 5):

$$FOM=\frac{\Delta\theta_r}{\Delta\theta_{HM}} \tag{5}$$

The FOM is often used as a weighted parameter that compromises the increase in the resonance shift and the deterioration in the measurement resolution. Although some researchers used different names (Jha and Sharma 2009), one can find the above definition in many works (Gent et al. 1990, Byun et al. 2007).

Evanescent field decay

The SPR phenomenon is accompanied by enhanced electromagnetic (EM) fields confined to the metal/analyte interface, which decay when they penetrate inside the metal and the analyte medium. The decay constant in each medium depends on the z-component of the K vector, which in turn depends on its permittivity. Due to the evanescent nature of the field, any variation in the analyte region results in a modification in the field distribution characteristics, which in fact constitute the sensing

mechanism. The correlation between the EM field distribution and the sensitivity was theoretically evaluated by Abdulhalim (2007) and recently verified experimentally (Shalabney and Abdulhalim 2010). The authors examined the correlation between the overlap integral of the EM intensity with the analyte region, and found that increasing the overlap integral means enhancing the sensitivity of the device. Figure 4 demonstrates the intensity distribution of the x- and z-components of the EM fields inside the metal and the analyte regions in the Kretschmann configuration. The calculations were done for 50 nm gold layer and 48 nm silver layer, which are the optimal thicknesses that satisfy the matching condition for each metal at λ=670 nm, giving the optimal conditions for the SPR phenomenon.

It can clearly be seen from Figure 4 that silver gives a sharper SPR dip with respect to gold, a smaller resonance angle (θ_r^{silver}=66.9°; θ_r^{gold}=70.2° for gold) and an enhanced EM field intensity of the z-component.

Dielectric overlayers

The discussion above corresponds to the basic configuration of a SPR sensor, composed of the prism and the metal layer. In practical devices, an additional ultrathin film of chromium or titanium is added beneath the metal layer in order to ensure the adhesion of the transducer metal layer to the glass slide (Figure 1). This layer, in fact, affects the sensor performances and tends to deteriorate some of the prominent characteristics. It is, however, primordial for the formation of stable and reusable SPR chips. Figure 5A shows the influence of a different thick titanium adhesion layer on the SPR signal. A broadening

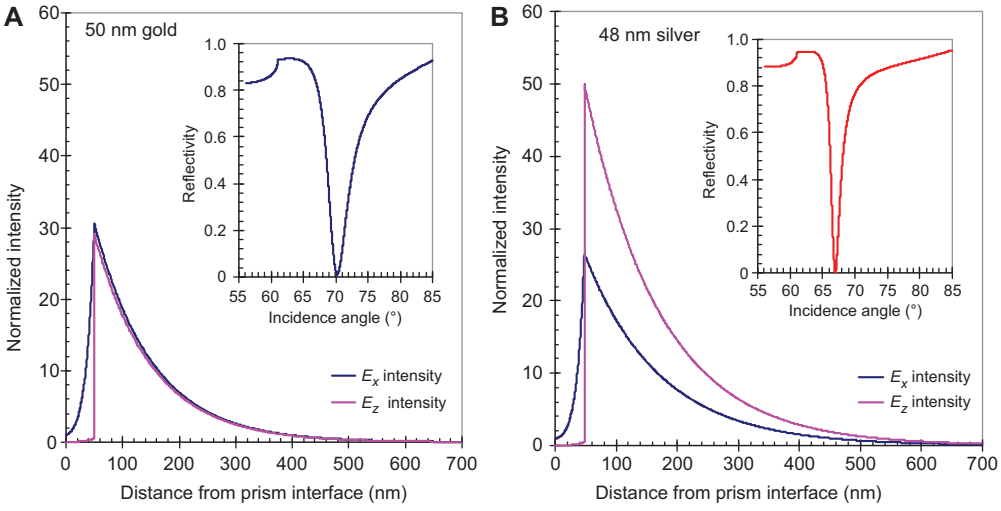

Figure 4 Electromagnetic field intensity distributions with increasing distance from the prism interface using Kretschmann configuration for: (A) 50 nm gold; and (B) 48 nm silver films. E_{xx} (blue) and E_z (pink): parameters used for calculations: n_{prism}=1.52, λ=670 nm, $n_{analyte}$=1.33. The insets present the reflectivity profiles for both cases.

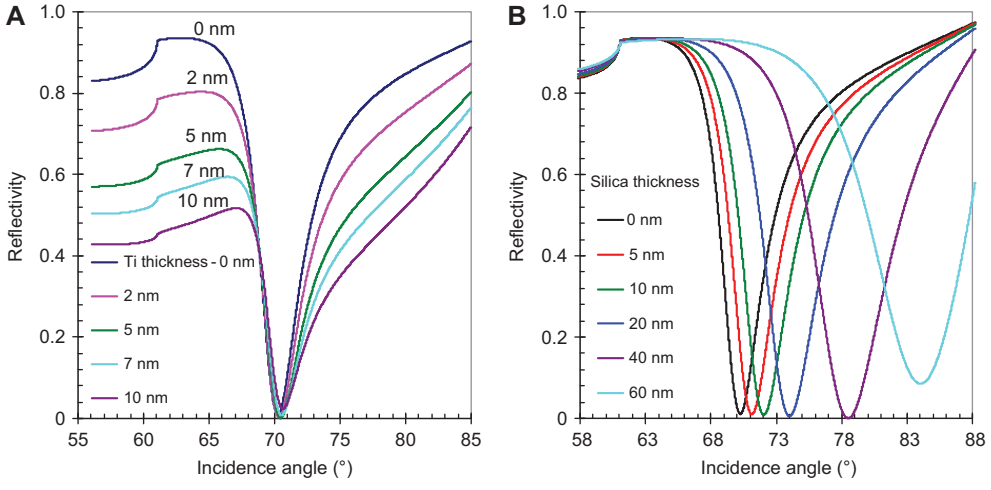

Figure 5 Influence of: (A) Ti adhesion layer between glass prism and metal film; and (B) silica top layer of different thickness on performances of SPR sensor; parameters used for calculations: n_{prism}=1.52, λ=670 nm, $n_{analyte}$=1.33, d_{gold}=50 nm, n_{silica}=1.48, d_{silica}=0–60 nm, $n_{titanium}$=2.32+3.08i, d_{Ti}=0–10 nm.

in the SPR dips and a decrease in the reflectance before the total internal reflection (TIR) regime are obtained. A wider SPR dip leads to less accuracy in determining the resonance angle, and smaller reflectance causes less contrast; both deteriorate the device performances. Adding a top dielectric layer, such as silica (n_{silica}=1.48), broadens the SPR dip, but does not decrease the depth, in particular for very thin silica films (Figure 5B).

One important aspect when considering such a multilayered SPR interface is the effect of the top dielectric layer on the sensitivity of the sensor. For this purpose, the effect of the silica layer thickness on the sensitivity was theoretically examined. From Figure 6A, where the angular sensitivity is presented next to the changes in the plasmonic resonance angle, one can see that the angular sensitivity improves with thicker silica coatings. For a silica thickness of d_{silica} ≈55 nm, the sensitivity becomes maximal, and thereafter dramatically deteriorates. The enhancement caused by the silica top layer with n_{silica}=1.48, can be considered moderate when compared to the enhancement caused by using a silicon top layer with a RI of $n_{silicon}$=3.75+0.017i. The angular sensitivity improvement in the case of a silica top layer is ≈30% for a 55 nm thick film, while it is ≈85% for a 4 nm silicon top-layer (Figure 6B).

Consequently, there is a strong interplay between thickness and RI of the nano-top overlayer, which will influence the sensitivity as well as the overall performance of the sensor. Several coatings will be considered in this review; each of these materials affects the SPR response in a different way. The characteristics of the coatings are defined based on the following criteria: (i) the possibility of forming experimentally stable layers on metal film at room temperature or at slightly elevated temperatures, (ii) having RIs between 1.33 and 3.75, (iii) showing insulating to conducting behavior, and (iv) allowing surface functionalization. The excitation wavelength was fixed at 670 nm and a prism of n_{prim}=1.52 was used throughout the work with a $n_{analyte}$ being water (n=1.33). The different materials considered are summarized in Table 1 comprising silica (SiO_x), antimony-doped tin oxide (SnO_2:Sb), ITO, diamond-like carbon (DLC) and amorphous carbonated silicon with a composition of a-$Si_{0.63}C_{0.37}$. In addition, a 10 nm thick silicon (Si) top-layer will be only theoretically considered. The resonance angle and the angular sensitivity were determined for a 10 nm thick overcoating, where the underlying gold film thickness was optimized to obtain the best SPR match. As a comparison, the angular sensitivity for a 50 nm gold film was included. Surprisingly, the angular sensitivity obtained for a silicon top layer is smaller than the other materials. This is due to the large thickness of the silicon layer used ($d_{silicon}$=10 nm). As shown in Figure 6B, a 4 nm Si overlayer shows a maximal angular sensitivity of ≈255°/RIU and drops drastically thereafter. The high real part of the silicon RI and small imaginary part at λ=670 nm ($n_{silicon}$=3.7563+0.0170i), are responsible for this behavior.

Having discussed theoretically the influence of the underlying metal film, the RI of the overcoating and its thickness, we will focus on the experimental results obtained on lamellar SPR structures.

Silicon oxide overcoating on gold

One of the first dielectric coatings experimentally investigated on SPR chips is glass-like coatings. This was motivated mainly by the fact that silicon dioxide-based materials, such as glass (silicate), are standard materials for biosensing, being inexpensive and benefiting from a rich variety of well-developed attachment schemes based on silane-coupling chemistry. Application of the knowledge on glass to SPR, enables the transfer of many existing protocols and commercial products

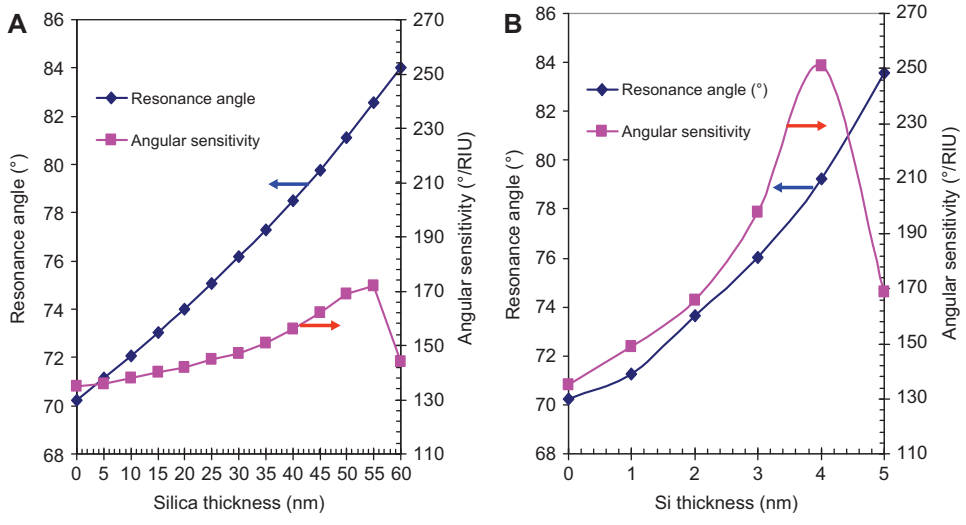

Figure 6 Change of angular sensitivity (pink) and position of resonance angle (blue) with different (A) silica; and (B) silicon top layers on gold thin films. Parameters used for calculations: n_{prism}=1.52, λ=670 nm, $n_{analyte}$=1.33, d_{gold}=50 nm, n_{silica}=1.48, d_{silica}=0–60 nm, $n_{silicon}$=3.75+0.017i, $d_{silicon}$=0–5 nm.

Table 1 Considered dielectric overlayers with their respective refractive indexes and theoretically calculated angular sensitivity when a 10 nm thick top dielectric layer was deposited onto an optimized gold film.

Dielectric overlayer	RI	Optimal gold layer thickness/(nm)	Resonance angle/(°)	Angular sensitivity (°/RIU)
SiO_x	1.48	49	72.28	139
SnO_2:Sb	1.91+0.249i	34	76.16	151
$Si_{0.63}C_{0.37}$	1.81+0.04i	44	75.89	175
ITO	2.00+0.001i	46	78.34	220
DLC	2.19+0.63i	26	77.33	126
Si	3.75+0.017i	19	88.44	77
Only gold	–	50	70.25	130

without significant efforts. In fact, a number of strategies developed on glass have already been adapted to gold substrate. However, adapting often proves to be a complex process, requiring time-consuming synthetic work and extensive manipulation of the existing protocols, to be effective on the new surface.

For many years, the development of gold/SiO_2 SPR interfaces was hampered, as the gold/SiO_2 interface was in most cases not stable upon immersion into water and PBS buffer and peeled off within a few minutes (Kambhampati et al. 2001). One successful strategy developed by Knoll and co-workers is based on a sol-gel approach. The silica films were 3–100 nm in thickness and further functionalization with amine and biotin modified silanes, introduced chemical functionalities onto the SPR interface. Cheng and co-workers proposed the formation of nanoscale silicate layers, by using layer-by-layer deposition of poly (allylamine hydrochloride) and sodium silicate, followed by calcination at high temperatures. This resulted in the formation of stable films of 2–15 nm in thickness (Phillips and Cheng 2007). The group of Kasemo demonstrated recently, that stable, smooth and very hydrophilic gold/SiO_2 interfaces can be prepared by spin coating poly(hydroxymethylsiloxane) onto the SPR chip, and post-treatment *via* plasma oxidation (Satriano et al. 2008, 2010). Our group deposited stable silica films directly on gold by using plasma-enhanced chemical vapor deposition (PECVD) (Szunerits and Boukherroub 2006a,b, Szunerits et al. 2006, 2008a, Zawisza et al. 2007, 2008). The technique is based on the decomposition of a mixture of silane gas (SiH_4) and nitrous oxide (N_2O) near the substrate surface, enhanced by the use of a vapor containing electrically charged particles or plasma at 300°C. The thickness and the RI of the silica layer are controlled by the reaction time and stoichiometry of the film. Silica coatings as thin as 7 nm with n=1.48, exhibited very good stability in both organic and aqueous solutions as well as in a piranha solution at 80°C. Figure 7 shows the effect of silica overlayers of different thicknesses deposited onto 50 nm gold film, with a 5 nm Ti adhesion layer, on the SPR characteristics. On the one hand, one can see clearly that increasing the SiO_x layer thickness (keeping the RI constant, n=1.48) shifts the resonance angle to higher values (Figure 7A,B), enhances the angular sensitivity of the plasmonic sensor chip (Figure 7B) which is maximal at ≈55 nm, and simultaneously increases the EM field intensity at the SiO_x/analyte interface (Figure 7C). On the other hand, increasing the silica thickness broadens the SPR dip and reduces the accuracy of the resonance measurements.

For sensing, the lamellar structure can be easily modified with functional silane molecules using the surface terminal Si-OH groups (Figure 8). It has been shown that the reaction with 3-aminopropyltrimethoxysilane (APTES) produces amine-terminal groups on the surface, where amine-terminated ligands, such as oligonucleotides, can be covalently linked *via* a bifunctional linker such as glutaraldehyde (Manesse et al. 2008b).

Antimony and indium tin oxide overcoatings on gold and silver films

While the formation of silica based SPR interface is easy and performable on a large scale, the deposition temperature of ≈300°C restricted its deposition onto gold only, as silver gets oxidized at this elevated temperature. SnO_2 and ITO thin films can be, however, deposited at room temperature. The formation of an antimony-doped tin oxide film (SnO_2:Sb) was carried out at room temperature using magnetron sputtering, using an antimony doped (5% and 2%) tin oxide target (Manesse et al. 2008a, 2009). Film thicknesses of 5 nm and higher could be deposited on silver and gold metal films, with a deposition rate of 2 nm/min (Manesse et al. 2008a, 2009). The presence of antimony resulted in thin films, with resistivity in the order of 10^{-4}–10^{-2} Ω cm (Manesse et al. 2008a, 2009) being largely more conductive than SiO_x overlayers. However, the Sb-doped SnO_2 overcoatings show optical properties, which are less favorable for SPR sensing (Manesse et al. 2008a, 2009). The imaginary part of the RI of these coatings is n=i0.249, which confers the Au/SnO_2:Sb composite interface a yellow color. This additional light absorption, as seen from experimentally determined SPR curves in Figure 9, results in a broadening of the SPR dip, and deteriorates the dip depth significantly.

Changing the underlying metal layer from gold to silver does not change the overall behavior. However, the angular sensitivity is significantly enhanced when comparing similar film thicknesses (Table 2).

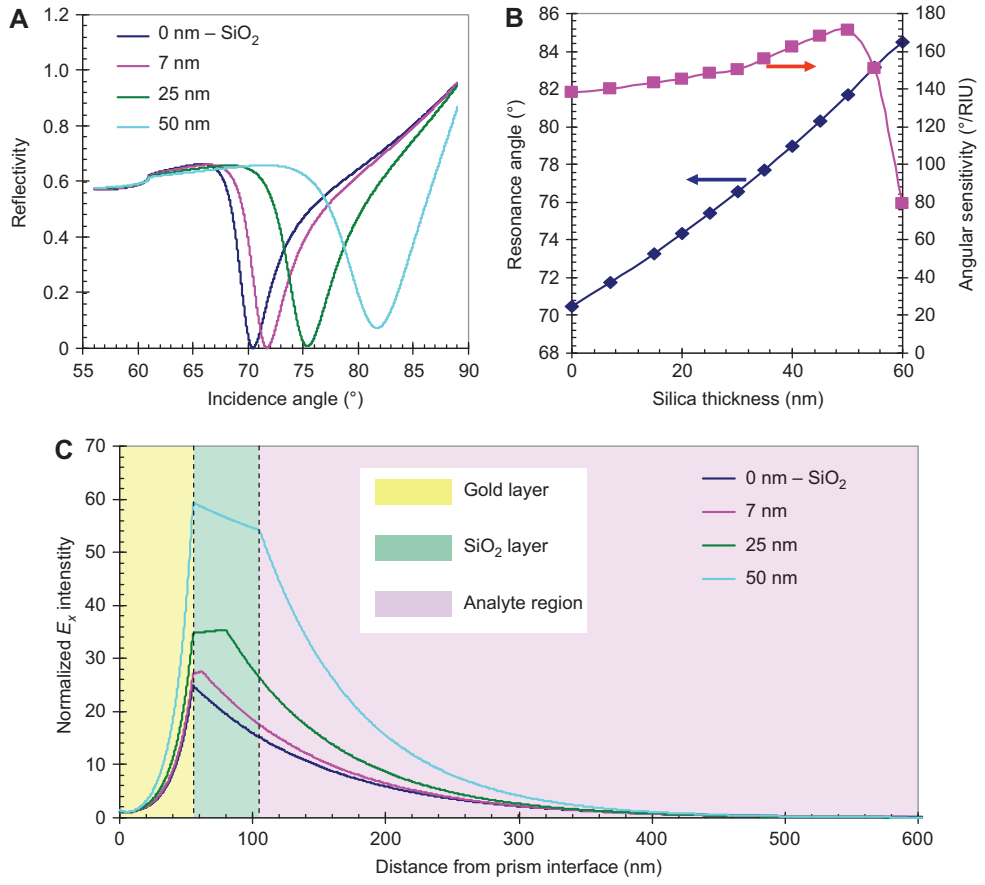

Figure 7 (A) Reflectivity response for different SiO_x overlayer thicknesses; (B) change of angular sensitivity (pink) and resonance angle (blue) vs. the SiO_x overlayer thickness; (C) E_x field intensity distribution normalized to the incident intensity as a function of the distance from prism interface for different SiO_x layer thicknesses; parameters used for calculations: n_{prism}=1.52, λ=670 nm, $n_{analyte}$=1.33, d_{gold}=50 nm, n_{silica}=1.48, n_{Ti}=2.32+3.08i, d_{Ti}=5 nm.

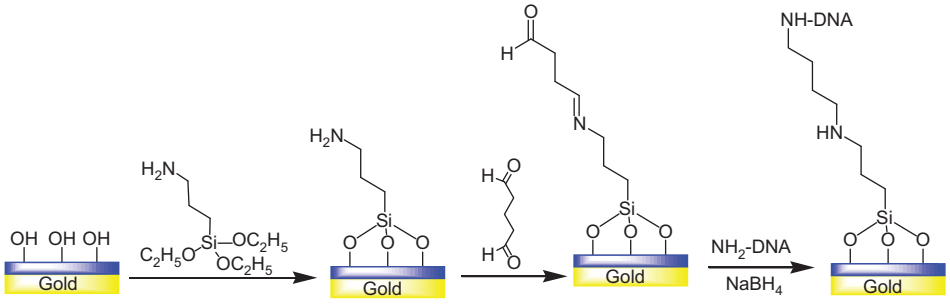

Figure 8 Schematic outline of the covalent linking of amine-terminated bioreceptors to silica coated SPR interfaces.

This problem of additional light absorption is less severe in the case of ITO overlayers. Different techniques can be used to synthesize ITO films, such as sol-gel processes, pulsed laser deposition and radio frequency (r.f.) sputtering (Mergel et al. 2001, Houng 2005, Kim et al. 2005, Szunerits et al. 2008b,c). In our case, r.f. sputtering using an In_2O_3-SnO_2 ceramic disk (90–10%) was performed at temperatures not exceeding 25°C, with a deposition rate of 0.6 nm/min. Under these conditions, the deposition of ITO layers onto silver thin films prevents silver from oxidation (Szunerits et al. 2008c). Figure 10 compares the SPR responses for a 10 nm ITO overlayer on gold and silver together with the EM field distribution. Using silver gives narrower SPR dips than those obtained using gold. On the other hand, the position of the resonance angle is at larger angles for gold, which is often a guarantee for higher sensitivity. Indeed, the angular

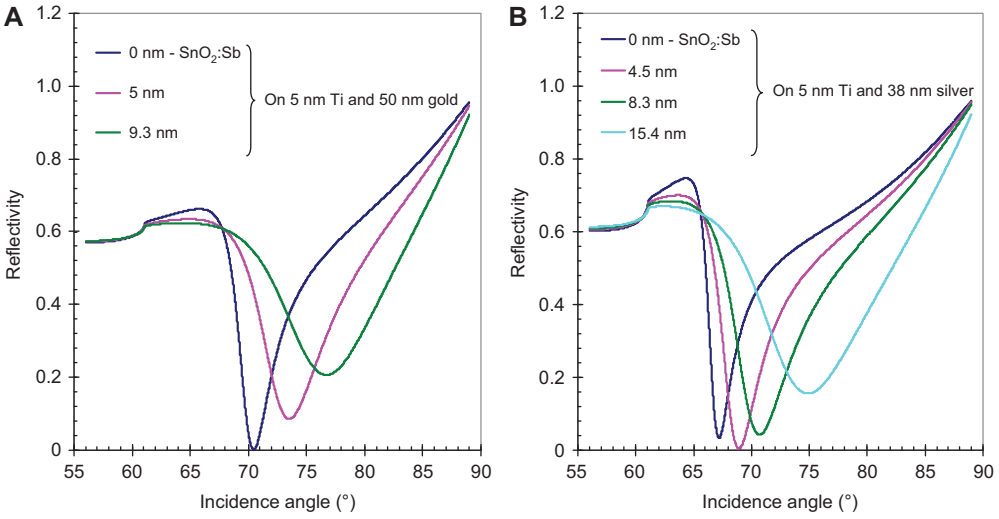

Figure 9 Influence of the SnO_2:Sb coating on the SPR performance: (A) deposited onto 50 nm gold; (B) deposited onto 38 nm silver; parameters used for calculations: n_{prism}=1.52, λ=670 nm, $n_{analyte}$=1.33, $n_{SnO_2/Sb}$=1.91+i0.2491, n_{Ti}=2.32+3.08i, d_{Ti}=5 nm.

Table 2 Angular sensitivity of 50 nm gold and 38 nm silver films coated with SnO_2:Sb of same thicknesses.

SnO_2:Sb layer Thickness (nm)	Resonance angle (°)		Angular sensitivity (°/RIU)	
	50 nm Gold	38 nm Silver	50 nm Gold	38 nm Silver
2	71.5	67.8	139	111
5	73.4	69.1	152	117
10	77.1	71.5	164	129

sensitivity of the gold (50 nm)/ITO structure is 233°/RIU while for the silver (38 nm)/ITO structure, the sensitivity is only 139°/RIU. The thickness of the underlying metal film influences strongly the angular sensitivity. Decreasing the gold thickness to 46 nm decreases the angular sensitivity to 220°/RIU.

Bioreceptors can be integrated on ITO and SnO_2:Sb interfaces in the same way as for silica-based lamellar structures (Manesse et al. 2009). It has been shown that surface carboxyl groups can be incorporated onto the surface using undecenyltrichlorosilane (UETS) in a two-step approach (Figure 11).

Amorphous carbonated silicon

A particularly interesting overcoating, is amorphous carbonated silicon (*a*-$Si_{1-x}C_x$:H). These films can be deposited using PECVD in a "low-power" regime, by employing methane gas as a carbon source and silane gas as a silicon supply (Solomon et al. 1988a,b). By varying the methane ratio in the gas

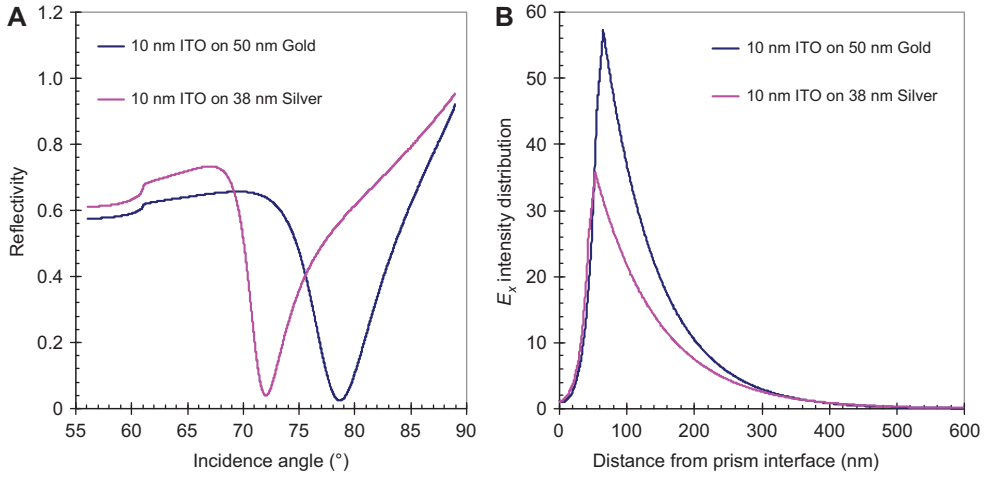

Figure 10 SPR (A) and EM fields calculations (B) for gold and silver based SPR interfaces with a 10 nm ITO overlayer; parameters used for calculations: n_{prism}=1.52, λ=670 nm, $n_{analyte}$=1.33, $n_{SnO_2/Sb}$=1.91+i0.2491, n_{Ti}=2.32+3.08i, d_{Ti}=5 nm.

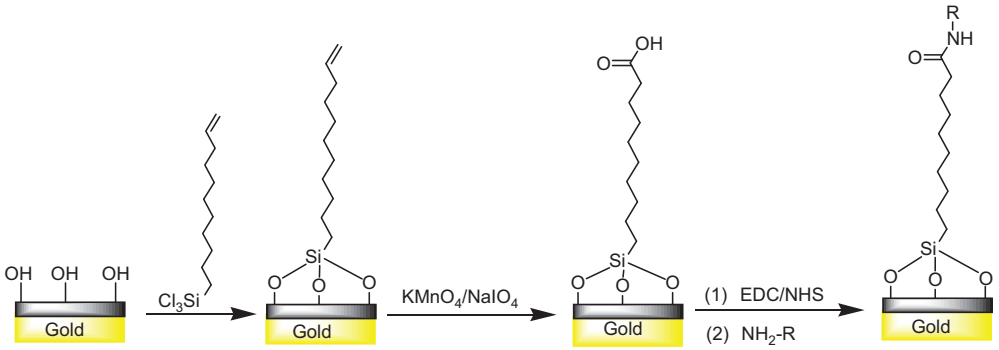

Figure 11 Schematic illustration of the carboxylation of oxide-based overlayers such as ITO and SnO_2:Sb.

mixture $[CH_4]/([SiH_4]+[CH_4])$, the final carbon (C) content in the material, and thus the optical properties, can be adjusted. For example, for the deposition of a-$Si_{0.63}C_{0.37}$:H, 94 at.% of $[CH_4]$ have to be used, while for an a-$Si_{0.80}C_{0.20}$:H film, only 51 at.% are necessary (Touahir et al. 2010a). Changing the carbon content of a-$Si_{1-x}C_x$:H additionally allows fine tuning of the RI of the material. A higher carbon content induces a decrease of the RI from n=2.51+i0.002 (a-$Si_{0.80}C_{0.20}$:H) to n=1.95+i0.03 (a-$Si_{0.67}C_{0.33}$:H) and n=1.81+i0.04 (a-$Si_{0.63}C_{0.37}$:H), respectively (Matsubara et al. 1990). Increasing the carbon content up to 37% widens the band gap further, but also increases the density of states in the band tails, resulting in an increase of the imaginary part of the RI. The effect on the SPR signal is shown in Figure 12. Changing the carbon content of a-$Si_{1-x}C_x$:H provides the ability to adjust the SPR dip location and width without varying the thickness. From the angular sensitivity aspect, the effect of the a-$Si_{1-x}C_x$:H is somehow similar to the previously discussed dielectric coatings. When the active metal layer is gold, the dip is wider and the sensitivity is higher. When silver is used, the dip is narrower and the sensitivity is smaller. The sensitivities for 50 nm gold layer coated with 5 nm thick a-$Si_{0.63}C_{0.37}$:H, a-$Si_{0.67}C_{0.33}$:H and a-$Si_{0.80}C_{0.20}$:H are 149, 156, and 183°/RIU, respectively. On the other hand, for 38 nm silver layer coated with the same layers, the corresponding sensitivities are 115, 117, and 127°/RIU, respectively.

The interest in a-$Si_{1-x}C_x$:H coatings arises additionally from the fact that well established surface functionalization strategies can be employed to form stable organic layers through robust Si-C covalent bonds, in a similar way as crystalline silicon (Boukherroub 2005). Indeed, while stable and reusable devices are formed using silanization, one of the drawbacks of silane chemistry is that it is not entirely well controlled. In addition, the Si-O-Si bonds are prone to hydrolysis when exposed to harsh environments, such as highly saline conditions. One approach used to anchor ligands to the lamellar SPR interface is shown in Figure 13. Surface-hydrogenated a-$Si_{0.63}C_{0.37}$:H films are immersed into undecylenic acid followed by UV irradiation, leading to the formation of an organic monolayer

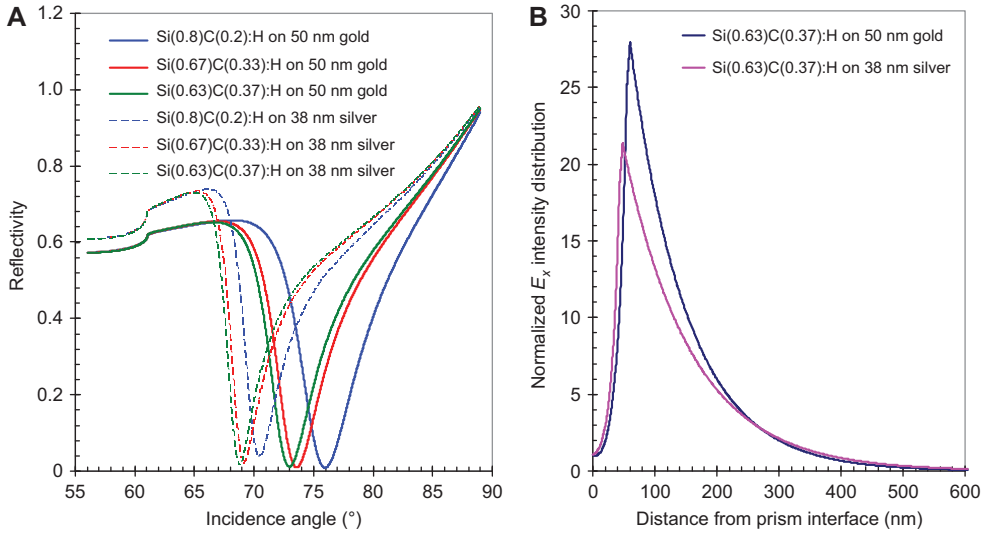

Figure 12 (A) Influence of carbon content of a 5 nm-thick a-$Si_{1-x}C_x$:H overlayer on gold (50 nm) and silver (38 nm); (B) E_x intensity distribution vs. distance from prism interface for both 50 nm gold and 38 nm silver films when it is coated with 5 nm a-$Si_{0.63}C_{0.37}$:H thin film; parameters used for calculations: n_{prism}=1.52, λ=670 nm, $n_{analyte}$=1.33, n_{Ti}=2.32+3.08i, d_{Ti}=5 nm, n($Si_{0.63}C_{0.37}$:H)=1.81+0.04i, n($Si_{0.67}C_{0.33}$:H=1.95+0.03i, n($Si_{0.80}C_{0.20}$:H)=2.51+0.002i.

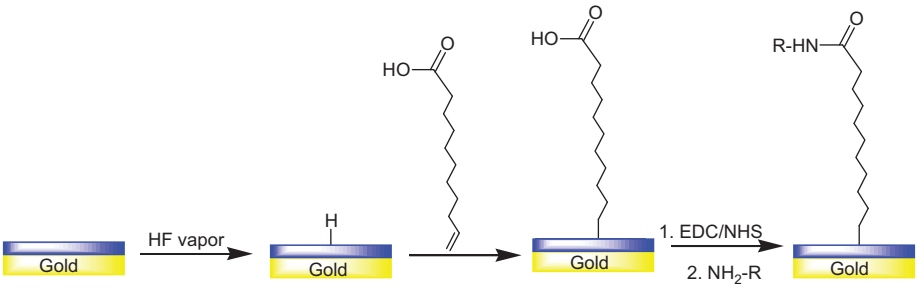

Figure 13 Surface hydrogenation of *a*-$Si_{1-x}C_x$:H thin film and subsequent functionalization with undecylenic acid.

covalently attached to the surface through Si-C bonds. From a quantitative infrared data analysis, a molecular density of linked carboxydecyl groups of $N_A \sim 2\times10^{13}$ mol cm^{-2} was calculated (Touahir et al. 2010a). This value is lower than that on crystalline silicon, as expected for a material incorporating a significant amount of methyl groups. The acid function can be further converted to an activated ester group using EDC/NHS chemistry, to which amine-terminated bioreceptors, such as biotin, DNA and (S)-N-(5-amino-1-carboxypentyl) iminodiacetic acid (NTA) can be easily anchored (Touahir et al. 2010a,b, Maalouli et al. 2011). An NTA modified SPR interface effectively chelated Cu^{2+} ions. Once loaded with metal ions, the modified SPR interface was able to bind specifically to histidine-tagged peptides. This interface was used in connection with a droplet-based SPR set to study the formation of a coordinative bond between surface linked NTA/Cu^{2+} and His_6-tagged peptides of different concentrations. The binding capacity is comparable with a Biacore NTA-chip, based on NTA-modified dextran layers. As it is generally more difficult for molecules to diffuse through such a hydrogel than to access a two-dimensional layer, the developed interface could be an interesting alternative when the analytes of interest are large molecules, and for kinetic parameter determination, when a low amount of non-specific binding is fundamental and low level of immobilization is recommended.

The use of a Ag/*a*-$Si_{0.63}C_{0.37}$:H (3 nm)/*a*-$Si_{0.80}C_{0.20}$:H (3 nm) interface, in connection with an optimized surface functionalization scheme, has been recently shown to allow for a highly sensitive analysis of interfacial DNA-DNA binding interactions using SPFS as a detection principle (Touahir et al. 2010b). It is well known, that the efficiency and kinetics for the hybridization reaction target DNA in solution with surface-confined DNA, is largely influenced by the steric accessibility and the rate of DNA diffusion from the bulk solution to the interface (Xu et al. 2008). Probe DNA crowding at the surface is thus a major factor affecting the hybridization efficiency. Mixed molecular layers can be easily grafted on *a*-$Si_{1-x}C_x$:H, by diluting the acid-anchoring groups necessary for DNA probe immobilization. This has been achieved by photochemical reaction in undecylenic acid in the presence of different concentrations of 1-decene. Surfaces with only 15% acid-anchoring groups proved to be optimal for sensitive SPFS sensing (Figure 14). On such interfaces, the resulting LOD≈500 fM, overcomes that of gold-based SPFS sensors, with the extra-advantage of benefiting from well-controlled processes for a robust covalent immobilization of biological probes on the substrate.

Diamond-like carbon overlayers

Diamond and most other forms of carbon, such as glassy carbon, carbon nanofibers and pyrolyzed films involve high temperature, often in the range of 800–1000°C, for growth deposition, limiting the ability to effectively integrate carbon with other materials. However, carbon also forms a range of less-crystalline materials, including DLC and other forms of amorphous carbon (*a*-C:H) films. Amorphous carbon is a particularly interesting material, as it can be deposited at room temperature (Sun et al. 2006, Akasaka et al. 2010). It can also be hydrogen-terminated using an inductively coupled hydrogen plasma, allowing the use of the same surface functionalization schemes developed for diamond (Szunerits and Boukherroub 2008). The elevated imaginary RI of DLC and *a*-C:H (n"=0.63i) makes it less favorable for SPR coatings.

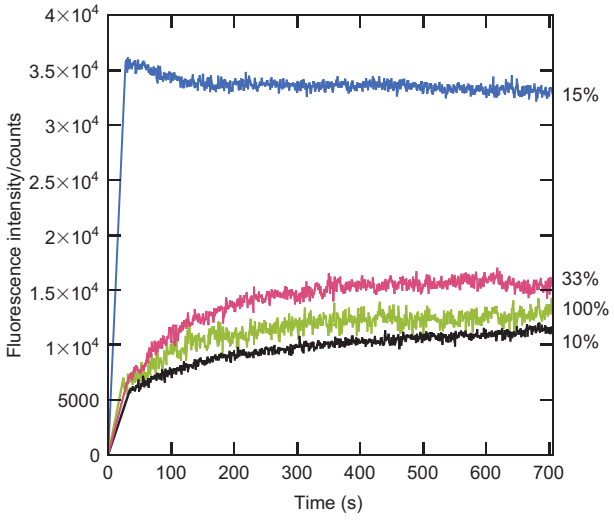

Figure 14 Influence of the concentration of acid-anchoring groups on the change of fluorescence intensity during hybridization of 5 nM complementary DNA targets in PBS with DNA probes immobilized from a 0.5 μM solution. Concentration of anchoring groups in the molecular layer: 100% (green); 33% (red); 15% (blue) and 10% (black).

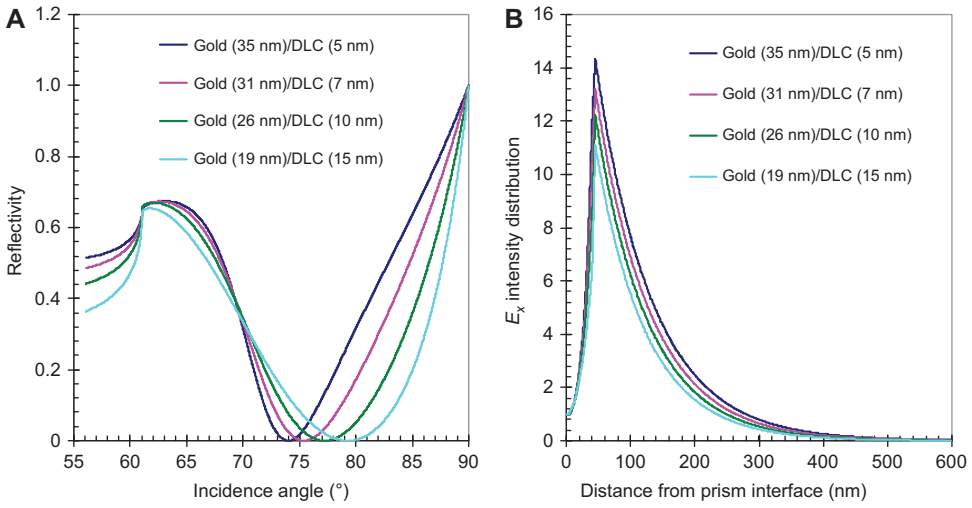

Figure 15 (A) Influence of amorphous carbon top layer thickness on the gold thin films on the SPR characteristics for several structures; (B) E_x intensity distribution of the same structures as in (A); parameters used for calculations: n_{prism}=1.52, λ=670 nm, $n_{analyte}$=1.33, n_{Ti}=2.32+3.08i, d_{Ti}=5 nm, n(DLC)=2.19+0.63i.

Figure 15 demonstrates the effect of depositing DLC layers above an optimal gold active layer, and the relationship between their thicknesses and the EM field distribution. Optimal, means the gold thickness that gives the minimum reflectivity in the resonance region, or what is known as full matching condition. For a DLC film of 10 nm thickness, the optimal gold layer thickness is 26 nm, while for a 15 nm DLC layer, the optimal gold layer is only 19 nm. Increasing the amorphous carbon film thickness requires thinner gold layers with smaller resonance angles. While minimum reflectivity is observed at the SPR angle, the SPR dips are very broad. Angular sensitivities are determined as 139°/RIU for a gold (35 nm)/DLC (5 nm) interface, 136°/RIU for gold (31 nm)/DLC (7 nm), 125°/RIU for gold (26 nm)/DLC (10 nm), and 94°/RIU for gold (19 nm)/DLC (15 nm).

This limited sensitivity might be the reason why there are currently only up to two reports on the integration of amorphous carbon with SPR chips. Lockett et al. (2008) deposited thin layers of amorphous carbon (0–20 nm) onto a surface plasmon active gold film, using a sputtering technique, and they used the resulting interfaces for the *in situ* synthesis of an oligonucleotide array utilizing photochemically protected oligonucleotide building blocks. In a related approach, different *a*-C:H layers (nitrogenated and fluorinated) were deposited onto a gold SPR interface by r.f. sputtering from a graphite target, in the presence of argon and an additional gas plasma of nitrogen or tetrafluoromethane (Akasaka et al. 2010). Here, the resistance to protein adsorption was studied.

Conclusions

Over the past years, extensive research has been devoted to the development of novel SPR sensors using multilayered structures. This paved the way towards the development of a variety of lamellar SPR interfaces, as described in this review. The fabrication of these interfaces would have, however, not been possible without the enormous progress made in the development of plasma-related deposition techniques. These methods have emerged as a key technology to tailor the surfaces of diverse materials. The advantages of these processes over chemical ones are associated to the wide range of possible experimental settings and changeable parameters. Controlling the gas flow rates, the gas ratio and the type of plasma, allows accurate tailoring of important film characteristics, such as the RI, the thickness and the extinction coefficient. The advantages of lamellar SPR interfaces are that they open the way to employ different innovative surface functionalization strategies, overcoming the low stability of Au-S bond. In addition, optimization of the film thickness, the RI together with the choice of the underlying metal where the SPR wave is propagating, allows tuning the position of the plasmon resonance angle and consequently the angular sensitivity. The higher the RI of the top nanodielectric layer, the higher the angular sensitivity. The optimal film thickness depends on the material and the wavelength used. One of the main challenges that faces SPR sensing in the coming years is, however, probably to widen the scope of commercially available SPR interfaces, so that people, not only specialists in surface chemistry, have access to the developed functionalization strategies widely employed in research laboratories. Although the number of sensing applications of SPR sensors is huge, as summarized in the tables given by Abdulhalim et al. (2008), a wider selection of interfaces will increase it even more.

Acknowledgments

The EU-ERDF via the Interreg IV programme (project “Plasmobio”), the Centre National de la Recherche Scientifique (CNRS), the Agence Nationale de la Recherche (ANR JCJC 2006) and the Nord-Pas-de Calais region are gratefully acknowledged for financial support. Prof. I. Abdulhalim would like to thank the financial support of the Singapore

National Research Foundation CREATE program 'Nanomaterials for Energy and Water Management' during the summer.

References

Abdulhalim, I. Biosensing configurations using guided wave resonant structures. In: NATO Science for Peace and Security Series B: Physics and Biophysics, Optical Waveguide Sensing and Imaging. Bock, W. J.; Gannot, I.; Tanev, S.; eds. Springer-Verlag: Amsterdam, 2007, Ch. 9, pp. 211–228. DOI:10.1007/978-1-4020-6952-9_9.

Abdulhalim, I.; Zourob, M.; Lakhtakia, A. Surface plasmon resonance for biosensing: a mini-review. *J. Electromag*. **2008**, *28*, 213.

Akasaka, H.; Gawazawa, N.; Suzuki, T.; Nakano, M.; Ohshio, S.; Saitoh, H. Evaluation of protein adsorption on hydrogenated amorphous carbon films by surface plasmon resonance phenomenon. *Diamond Relat. Mater.* **2010**, *19*, 1235.

Alleyne, C. J.; Kirk, A. G.; McPhedran, R. C.; Nicorovici, N.-A. P.; Maystre, D. Enhanced SPR sensitivity using periodic metallic structures. *Optics Express* **2007**, *15*, 8163–8169.

Boukherroub, R. Chemical reactivity of hydrogen-terminated crystalline silicon surfaces. *Curr. Opin. Solid State Mater. Sci.* **2005**, *9*, 66.

Byun, K. M.; Kim, S. J.; Kim, D. Grating-coupled transmission-type surface plasmon resonance sensors based on dielectric and metallic gratings. *Applied Optics* **2007**, *46*, 5703–5708.

Chabot, V.; Cuerrier, C. M.; Escher, E.; Aimez, V.; Grandbois, M.; Charette, P. G. Biosensing based on surface plasmon resonance and living cells. *Biosens. Bioelectron.* **2009**, *24*, 1667–1673.

Dostalek, J.; Knoll, W. Biosensors based on surface plasmon-enhanced fluorescence spectroscopy (Review). *Biointerphases* **2008**, *3*, FD12.

Franzen, S. Surface plasmon polaritons and screened plasma absorption in indium tin oxide compared to silver and gold. *J. Phys. Chem. C.* **2008**, *112*, 6027.

Gent, J. V.; Lambeck, P.; Kreuwel, H.; Gerritsma, G.; Sudholter, E.; Reinhoudt, D.; Popma, T. Optimization of a chemooptical surface plasmon resonance based sensor. *Appl. Optics* **1990**, *29*, 2843–2849.

Gupta, G.; Kondoh, J. Tuning and sensitivity enhancement of surface plasmon resonance sensor. *Sens. Actuat. B* **2007**, *122*, 381–388.

He, L.; Musick, M. D.; Nicewarner, S. R.; Salinas, F. G.; Benkovic, S. J.; Natan, M. J.; Keating, C. D. Colloidal Au-enhanced surface plasmon resonance for ultrasensitive detection of DNA hybridization. *J. Am. Chem. Soc.* **2000**, *122*, 9071–9077.

Houng, B. Tin doped indium oxide transparent conducting thin films containing silver nanoparticles by sol-gel technique. *Appl. Phys. Lett.* **2005**, *87*, 251922.

Jha, R.; Sharma, A. K. Chalcogenide glass prism based SPR sensor with Ag–Au bimetallic nanoparticle alloy in infrared wavelength region. *J. Opt. A: Pure Appl. Opt.* **2009**, *11*, 045502.

Jory, M. J.; Vukusic, P. S.; Sambles, J. R. Development of a prototype gas sensor using surface plasmon resonance on gratings. *Sens. Actuators B* **1994**, *17*, 203–209.

Kabashin, A. V.; Nikitin, P. I. Surface plasmon resonance interferometer for bio- and chemical-sensors. *Opt. Commun.* **1998**, *150*, 5–8.

Kabashin, A. V.; Evans, P.; Pastkovsky, S.; Hendren, W. A.; Wurtz, G.; Atkinson, R.; Pollard, R.; Podolskiy, V. A.; Zayats, A. V. Plasmonic nanorod metamaterials for biosensing. *Nature Mater.* **2009**, *8*, 867–871.

Kambhampati, D. K. M.; Robertson, J. W.; Cai, M.; Pemberton, J. E.; Knoll, W. Novel silicon dioxide sol-gel films for potential sensor applications: a surface plasmon resonance study. *Langmuir* **2001**, *17*, 1169–1175.

Karabchevsky, A.; Karabchevsky, S.; Abdulhalim, I. Nanoprecision algorithm for surface plasmon resonance determination from images with low contrast for improved sensor resolution. *J. NanoPhoto* **2011a**, *5*, DOI: 10.1117/1.3598138.

Karabchevsky, A.; Karabchevsky, S.; Abdulhalim, I. Fast surface plasmon resonance imaging sensor using radon transform. *Sens. Actuators B: Chemical* **2011b**, *155*, 361–365.

Karlsson, R.; Stahlberg, P. Surface plasmon resonance detection and multispot sensing for direct monitoring of interactions involving low-molecular-weight analytes and for determination of low affinities. *Anal. Biochem.* **1995**, *228*, 274.

Kim, S. H.; Park, N. M.; Kim, T. Y.; Sung, G. Y. Electrical and optical characteristics of ITO films by pulsed laser deposition using a 10 wt.% SnO_2-doped In_2O_3 ceramic target. *Thin Solid Films* **2005**, *475*, 262.

Lahav, A.; Auslender, M.; Abdulhalim, I. Sensitivity enhancement of guided-wave surface-plasmon resonance sensors. *Opt. Lett.* **2008**, *33*, 2539–2541.

Lahav, A.; Shalabaney, A.; Abdulhalim, I. Surface plasmon sensor with enhanced sensitivity using top nano dielectric layer. *J. Nanophotonics* **2009**, *3*, 031501.

Lee, J.-Y.; Shih, H.-C.; Hong, C.-T.; Chou, T. K. Measurement of refractive index change by surface plasmon resonance and phase quadrature interferometry. *Opt. Commun.* **2007** *276*, 283–287.

Linman, M. J.; Sugerman, K.; Cheng, Q. Detection of low levels of Escherichia coli in fresh spinach by surface plasmon resonance spectroscopy with a TMB-based enzymatic signal enhancement method. *Sens. Actuators B* **2010**, *145*, 613–619.

Liu, H.; Wang, B.; Leong, E. S. P.; Yang, P.; Zong, Y.; Si, G.; Teng, J.; Maier, S. A. Enhanced surface plasmon resonance on a smooth silver film with a seed growth layer. *ACS Nano* **2010**, *4*, 3139.

Lockett, M. R.; Weibel, S. C.; Philips, M. F.; Shortreed, M. R.; Sun, B.; Corn, R. M.; Hamers, R. J.; Cerrina, F.; Smith, L. M. Carbon-on-metal films for surface plasmon resonance detection of DNA arrays. *J. Am. Chem. Soc*. **2008**, *130*, 8611–8613.

Maalouli, N.; Gouget-Laemmel, A. C.; Pinchemel, B.; Bouazaoui, M.; Chazalviel, J. N.; Ozanam, F.; Yang, Y.; Burkhard, P.; Boukherroub, R.; Szunerits, S. Development of a metal-chelated plasmonic interface for the linking of his-peptides with a droplet-based surface plasmon resonance read-off scheme. *Langmuir* **2011**, *27*, 5498.

Manesse, M.; Sanjines, R.; Stambouli, V.; Boukherroub, R.; Szunerits, S. Preparation and characterization of antimony-doped SnO_2 thin films on gold and silver substrates for electrochemical and surface plasmon resonance studies. *Electrochem. Commun.* **2008a**, *10*, 1041.

Manesse, M.; Stambouli, V.; Boukherroub, R.; Szunerits, S. Electrochemical impedance spectroscopy and surface plasmon resonance studies of DNA hybridization on gold/SiOx interfaces. *Analyst* **2008b**, *133*, 1097–1103.

Manesse, M.; Sanjines, R.; Stambouli, V.; Boukherroub, R.; Szunerits, S. Preparation and characterization of silver substrates coated with antimony-doped SnO_2 thin films for surface plasmon resonance studies. *Langmuir* **2009**, *25*, 8036.

Masale, M. The theory of attenuated total reflection by surface polaritons on one-sided corrugated thin films. *Physica B* **2003**, *325*, 385–393.

Matsubara, K.; Kawata, S.; Minami, S. Multilayer system for a high-precision surface plasmon resonance sensor. *Opt. Lett.* **1990**, *15*, 75–77.

Mazumdara, S. D.; Barlena, B.; Kämpferb, P.; Keusgen, M. Surface plasmon resonance (SPR) as a rapid tool for serotyping of Salmonella. *Biosens. Bioelectron.* **2010**, *25*, 967–971.

Mergel, D.; Schenkel, M.; Ghebre, M.; Sulkowski, M. Structural and electrical properties of In_2O_3:Sn films prepared by radio-frequency sputtering. *Thin Solid Films* **2001**, *392*, 91.

Meunier, M.; Prasad, P. N.; Kabashin, A. V.; Patskovsky, S. Self-noise-filtering phase-sensitive surface plasmon resonance biosensing. *Optics Express* **2010**, *18*, 14353–14358.

Phillips, K. S.; Cheng, Q. Recent advances in surface plasmon resonance based techniques for bioanalysis. *Anal. Bioanal. Chem.* **2007**, *387*, 1831.

Raether, H. Surface Plasmon on Smooth and Rough Surfaces and on Gratings. Springer-Verlag: New York, USA, 1988.

Sarid, D.; Deck, R. T.; Craig, A. E.; Hickernell, R. K.; Jameson, R. S.; Fasano, J. Optical field enhancement by long-range surface-plasma waves. *J. Appl. Opt.* **1982**, *21*, 3993–3995.

Satriano, C.; Marletta, G.; Kasemo, B. Oxygen plasma-induced conversion of polysiloxane into hydrophilic and smooth SiOx surfaces. *Surf. Interface Anal.* **2008**, *40*, 649.

Satriano, C.; Edvardsson, M.; Ohlsson, G.; Wang, G.; Svedhem, S.; Kasemo, B. Plasma oxidized polyhydroxymethylsiloxane – a new smooth surface for supported lipid bilayer formation. *Langmuir* **2010**, *26*, 5715–5725.

Schasfoort, R. B. M.; Tudos, A. J. Handbook of Surface Plasmon Resonance. The Royal Society of Chemistry, 2008.

Schroter, U.; Heitmann, D. Grating couplers for surface plasmons excited on thin metal films in the Kretschmann-Raether configuration. *Phys. Rev. B* **1999**, *60*, 4992–4999.

Shalabney, A.; Abdulhalim, I. Electromagnetic fields distribution in multilayer thin film structures and the origin of sensitivity enhancement in surface plasmon resonance sensors. *Sens. Actuators A* **2010**, *159*, 24–32.

Shalabney, A.; Abdulhalim, I. Sensitivity-enhancement methods for surface plasmon sensors. *Laser Photonics Rev.* **2011**, *5*, 571–606.

Shalabney, A.; Lakhtakia, A.; Abdulhalim, I.; Lahav, A.; Patzig, C.; Hazek, I.; Karabchevsky, A.; Rauschenbach, B.; Zhang, F.; Xu, J. Surface plasmon resonance from metallic columnar thin films. *Photonics and Nanostructures – Fundamentals and Applications* **2009**, *7*, 176–185.

Shalabney, A.; Khare, C.; Rauschenbach, B.; Abdulhalim, I. Sensitivity of surface plasmon resonance sensors based on metallic columnar thin films in the spectral and angular interrogations. *Sens. Actuat. B* **2011**, *151*, 201–212.

Slavik, R.; Homola, J. Ultrahigh resolution long range surface plasmon-based sensor. *Sens. Actuators B* **2007**, *123*, 10–12.

Solomon, I.; Schmidt, M. P.; Tran-Quoc, H. Selective low-power plasma decomposition of silane-methane mixtures for the preparation of methylated amorphous silicon. *Phys. Rev. B* **1988a**, *38*, 9895.

Solomon, I.; Schmidt, M. P.; Sénémaud, C.; Driss Khodja, M. Band structure of carbonated amorphous silicon studied by optical, photoelectron, and x-ray spectroscopy. *Phys. Rev. B* **1988b**, *38*, 13263.

Sun, B.; Colavita, P. E.; Kim, H.; Lockett, M.; Marus, M. S.; Smith, L. M.; Hamers, R. J. Covalent photochemical functionalization of amorphous carbon thin films for integrated real-time biosensing. *Langmuir* **2006**, *22*, 9598.

Szunerits, S.; Boukherroub, R. Electrochemical investigation of gold/silica thin film interfaces for electrochemical surface plasmon resonance studies. *Electrochem. Commun.* **2006a**, *8*, 439–444.

Szunerits, S.; Boukherroub, R. Preparation and characterization of thin films of SiO_x on gold substrates for surface plasmon resonance studies. *Langmuir* **2006b**, *22*, 1660.

Szunerits, S.; Boukherroub, R. Different strategies for functionalization of diamond surfaces. *J. Solid State Electrochem.* **2008**, *12*, 1205–1218.

Szunerits, S.; Coffinier, Y.; Janel, S.; Boukherroub, R. Stability of the gold/silica thin film interface: electrochemical and surface plasmon resonance studies. *Langmuir* **2006**, *22*, 10716–10722.

Szunerits, S.; Nunes-Kirchner, C.; Wittstock, G.; Boukherroub, R.; Chantal, G. Electrochemical investigations of the influence on the thickness of thin films of SiOx on gold substrates on charge transfer characteristics. *Electrochim. Acta* **2008a**, *53*, 7805–7914.

Szunerits, S.; Castel, X.; Boukherroub, R. Preparation of electrochemical and surface plasmon resonance active interfaces: deposition of indium tin oxide on silver thin films. *J. Phys. Chem. C.* **2008b**, *112*, 10883.

Szunerits, S.; Castel, X.; Boukherroub, R. Surface plasmon resonance investigation of silver and gold films coated with thin indium tin oxide layers: influence on stability and sensitivity. *J. Phys. Chem. C.* **2008c**, *112*, 15813–15817.

Touahir, L.; Niedziółka-Jönsson, J.; Galopin, E.; Boukherroub, R.; Gouget-Laemmel, A. C.; Solomon, I.; Petukhov, M.; Chazalviel, J.-N.; Ozanam, F.; Szunerits, S. Surface plasmon resonance on gold and silver films coated with thin layers of amorphous silicon–carbon alloys. *Langmuir* **2010a**, *26*, 6058.

Touahir, L.; Jenkins, A. T. A.; Boukherroub, R.; Gouget-Laemmel, A. C.; Chazalviel, J.-N.; Peretti, J.; Ozanam, F.; Szunerits, S. Surface plasmon-enhanced fluorescence spectroscopy on silver based SPR substrates. *J. Phys. Chem. C.* **2010b**, *114*, 22582.

Vala, M.; Etheridge, S.; Roach, J.; Homola, J. Long-range surface plasmons for sensitive detection of bacterial analytes. *Sens. Actuators B* **2009**, *139*, 59–63.

Wang, L.; Sun, Y.; Wang, J.; Zhu, X.; Jia, F.; Cao, Y.; Wang, X.; Zhang, H.; Song, D. Sensitivity enhancement of SPR biosensor with silver mirror reaction on the Ag/Au film. *Talanta* **2009**, *78*, 265.

Xu, F.; Pellino, A. M.; Knoll, W. Electrostatic repulsion and steric hindrance effects of surface probe density on deoxyribonucleic acid (DNA)/peptide nucleic acid (PNA) hybridization. *Thin Solid Films* **2008**, *516*, 8634–8639.

Yao, D. F.; Yu, F.; Kim, J. Y.; Scholz, J.; Nielsen, P. E.; Sinner, E. K.; Knoll, W. Surface plasmon field-enhanced fluorescence spectroscopy in PCR product analysis by peptide nucleic acid probes. *Nucleic Acid. Res.* **2004**, *32*, 177.

Yuan, X.-C.; Ong, B. H.; Tan, Y. G.; Zhang, D. W.; Irawan, R.; Tjin, S. C. Sensitivity–stability-optimized surface plasmon resonance sensing with double metal layers. *J. Opt. A: Pure Appl. Opt.* **2006**, *8*, 959.

Yuk, J. S.; Hong, D. G.; Jung, J. W.; Jung, S. H.; Kim, H. S.; Han, J. A.; Kim, Y. M.; Ha, K. S. Sensitivity enhancement of spectral surface plasmon resonance biosensors for the analysis of protein arrays. *Eur. Biophys. J.* **2006**, *35*, 469–476.

Zawisza, I.; Wittstock, G.; Boukherroub, R.; Szunerits, S. PM IRRAS investigation of thin silica films deposited on gold. Part 1. Theory and proof of concept. *Langmuir* **2007**, *23*, 9303–9309.

Zawisza, I.; Wittstock, G.; Boukherroub, R.; Szunerits, S. Polarization modulation infrared reflection absorption spectroscopy investigations of thin silica films deposited on gold. 2. Structural analysis of 1,2-dimyristoyl-sn-glycero-3-phosphocholine bilayer. *Langmuir* **2008**, *24*, 3922–3929.

Zhaoming, Z.; Brown, T. G. Nonperturbative analysis of cross coupling in corrugated metal films. *J. Opt. Soc. Am. A* **2000**, *17*, 1798–1806.

Zynio, S. A.; Samoylov, A. V.; Surovtseva, E. R.; Mirsky, V. M.; Shirshov, Y. M. Bimetallic layers increase sensitivity of affinity sensors based on surface plasmon resonance. *Sensors* **2002**, *2*, 62.

Received September 12, 2011; accepted October 25, 2011;
previously published online December 13, 2011